6 EULERIAN DISPERSION MODELS

Air pollution diffusion can be numerically simulated by several techniques, which are mainly divided into two categories:

1. Eulerian models
2. Lagrangian models

Each of these has advantages and disadvantages in the treatment of atmospheric phenomena. Several authors, and in particular Lamb (from Longhetto, 1980), have investigated the two approaches and their interrelationships in detail, as outlined in Figure 6–1.

The basic difference between the Eulerian and Lagrangian view is illustrated in Figure 6–2, in which the Eulerian reference system is fixed (e.g., with respect to the earth) while the Lagrangian reference system follows the average atmospheric motion.

This section presents the fundamentals of the Eulerian approach and the major Eulerian modeling techniques for atmospheric diffusion. Lagrangian methods are discussed in Chapter 8, while Gaussian dispersion models, which can be seen as both Eulerian and Lagrangian, are presented in Chapter 7. A discussion of the methodologies that have been used to evaluate dispersion models against measurements is presented in Section 12.5.

6.1 THE EULERIAN APPROACH

The Eulerian approach is based (Lamb, from Longhetto, 1980) on the conservation of mass of a single pollutant species of concentration $c(x,y,z,t)$.

$$\frac{\partial c}{\partial t} = -\mathbf{V} \cdot \nabla c + D \nabla^2 c + S \qquad (6\text{–}1)$$

which is similar to Equation 4–7 for the conservation of water, but has the additional (often negligible) molecular diffusion term $D \nabla^2 c$, where D is the molecular diffusivity (about $1.5 \cdot 10^{-5}$ m^2 s^{-1} for air), $\nabla^2 = \partial^2/\partial x^2 + \partial^2/\partial y^2 + \partial^2/\partial z^2$ is the Laplacian operator, and ∇ is the gradient operator.

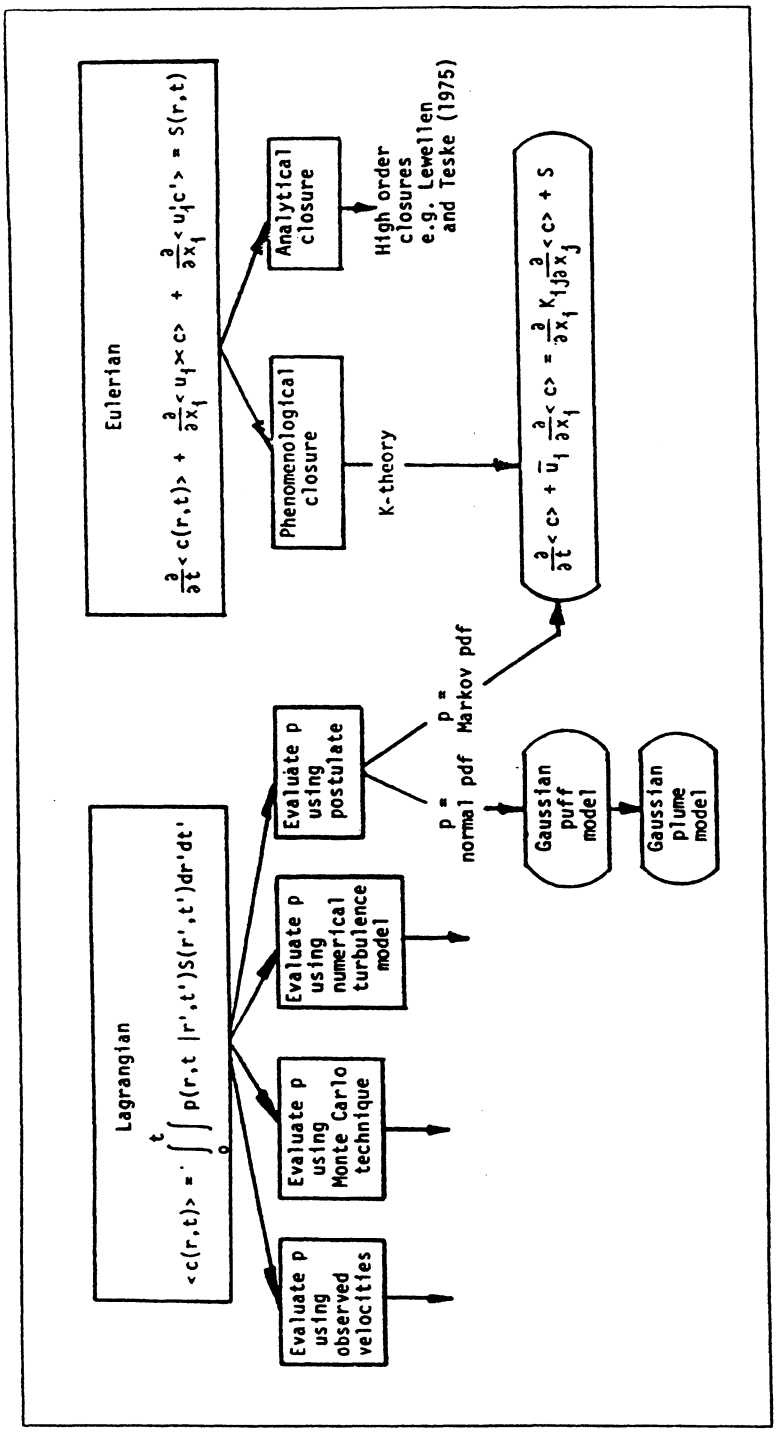

Figure 6–1. Schematic illustration of relationships among the Eulerian and Lagrangian models of turbulent diffusion (from Lamb, in Longhetto, 1980). [Reprinted with permission from Elsevier.]

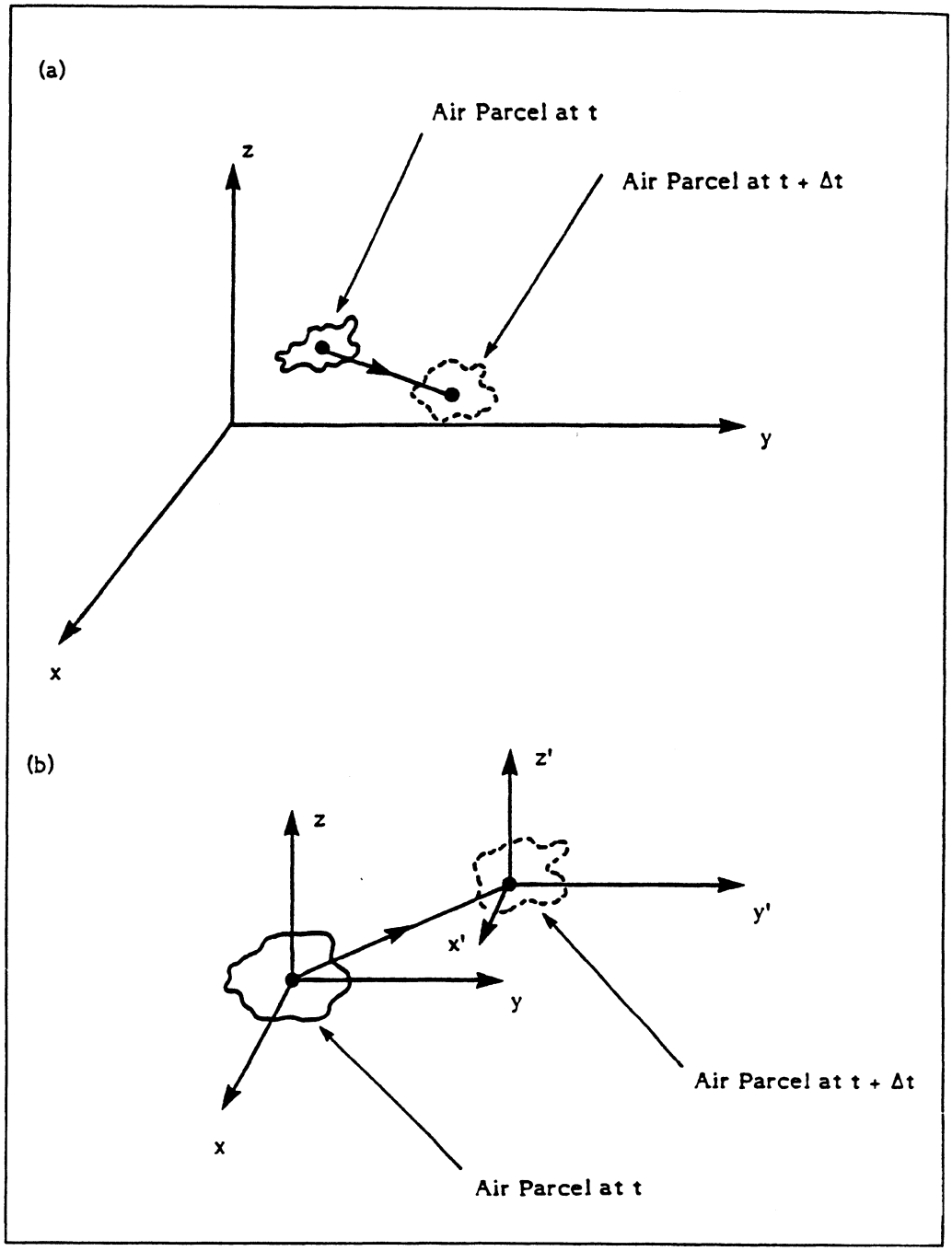

FIGURE 6–2. Eulerian (a) and Lagrangian (b) reference systems for the atmospheric motion.

We assume that the velocity **V** can be represented as the sum of "average" and "fluctuating" components, i.e.

$$\mathbf{V} = \bar{\mathbf{u}} + \mathbf{u}' \tag{6-2}$$

where $\bar{\mathbf{u}}$ represents the portion of the flow that is resolvable using measurements or meteorological models, and $\mathbf{u}'$ is the remaining unresolvable component. We also assume

$$c = \langle c \rangle + c' \tag{6-3}$$

where $\langle\ \rangle$ denotes the ensemble (theoretical) mean, whose meaning is clarified below. Then, substituting Equations 6-2 and 6-3 in 6-1 and taking the ensemble average, we obtain

$$\frac{\partial \langle c \rangle}{\partial t} = - \bar{\mathbf{u}} \cdot \nabla \langle c \rangle - \nabla \cdot \langle c' \mathbf{u}' \rangle + D \nabla^2 \langle c \rangle + \langle S \rangle \tag{6-4}$$

in which, according to the ergodic hypothesis, it is assumed that $\langle \bar{\mathbf{u}} \rangle = \bar{\mathbf{u}}$ and $\langle \mathbf{u}' \rangle = \mathbf{0}$.

Meteorological models have a large unresolved portion $\mathbf{u}'$, which is often of the same order of magnitude as $\bar{\mathbf{u}}$. Therefore, the term $\langle c'\mathbf{u}' \rangle$ is very large and contains most of the turbulent atmospheric diffusion eddies, whose dispersion effects are orders of magnitude larger than the molecular ones. Even with a perfect meteorological model providing detailed information about $\bar{\mathbf{u}}(x,y,z,t)$ (i.e., $\bar{\mathbf{u}} \simeq \mathbf{V}$), the spatial and temporal scales of the smaller turbulent eddies are so small that a correct numerical integration of Equation 6-4 would be practically impossible (it would probably require a grid size of about 1 mm in the entire computational domain; Wyngaard, from Nieuwstadt and van Dop, 1982).

The understanding of $\mathbf{u}'$ as an unresolvable component that can be minimized but never eliminated is the key to understanding the significance of ensemble averaging. Lamb (from Longhetto, 1980) clarifies this point by noting that $\mathbf{u}'$ is a stochastic variable; i.e., there exists an infinite family of functions $\mathbf{u}'$ that satisfy the equation of motion. The situation is described in Figure 6-3, where each possible member $\mathbf{u}'$ of the family generates a different concentration c. The average, at a certain point and time, of all possible concentrations generated by the different $\mathbf{u}'$ gives the "theoretical" ensemble mean $\langle c \rangle$. Naturally, if we could measure $\mathbf{u}'$ and c continuously and everywhere, we could evaluate the exact member of the family that has occurred in reality. Lacking this information, we

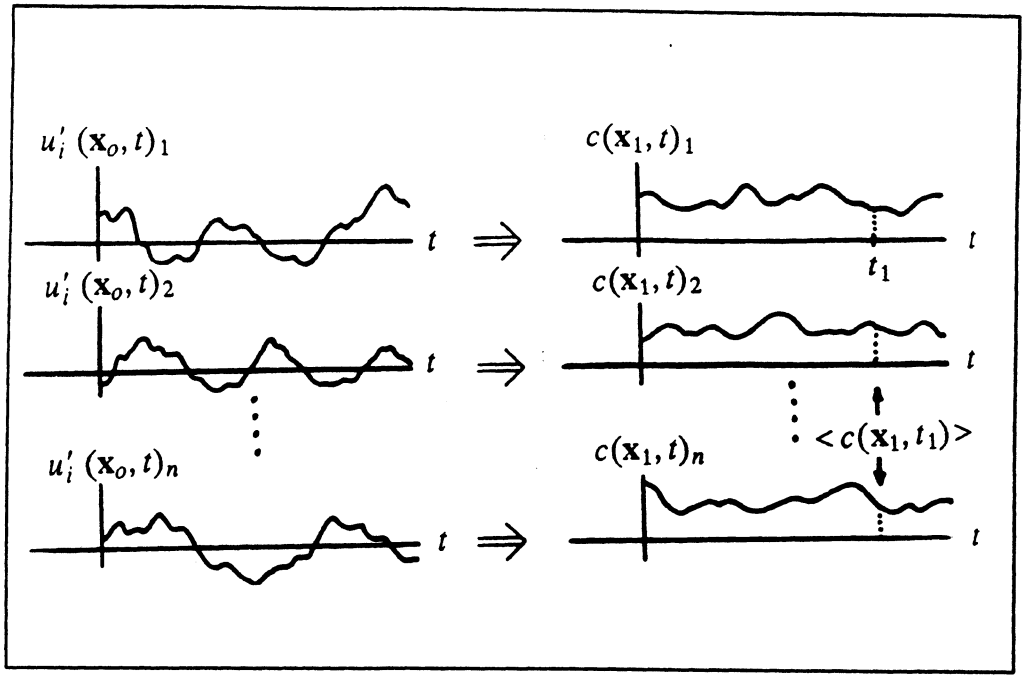

Figure 6–3. The infinite family or ensemble of velocity functions u_i' and the corresponding family of concentration distributions, each portrayed at fixed points $\mathbf{x}_o$ and $\mathbf{x}_1$ as functions of time. The subscript n, n=1,2... , denotes the member or realization of the ensemble. The ensemble mean value <c> at a given time t_1 is formed by averaging $c(\mathbf{x}, t_1)_n$ over the infinite ensemble, as indicated by the vertical dashed line (adapted from Lamb; in Longhetto, 1980).

must assume that all theoretically acceptable $\mathbf{u}'$ are equally possible, thus allowing, in the best possible conditions, the computation of <c> instead of the actual c.

An important conclusion is that the output <c> provided by all Eulerian models is conceptually different from the air quality data gathered from monitoring activities. In fact, monitoring data provide estimates of the actual concentration c (with a certain degree of error associated with the monitoring technique), while model outputs are estimates of <c> (with a certain degree of error because of the input data and the numerical and/or analytical approximations). Therefore, even during ideal conditions (i.e., with no monitoring and modeling errors) model outputs will still differ from concentration measurements. This is often called the intrinsic (unremovable) uncertainty in dispersion modeling.

Another important point can be derived from the analysis of the term $\nabla \cdot \langle c'\mathbf{u}' \rangle$ in Equation 6-4. This term introduces three new unknowns. Therefore, the solution of Equation 6-4 requires a relation between the meteorological input terms or the average terms <c> and these three additional unknowns. The simplest approximation (phenomenological closure) is given by the so-called *K*-theory or gradient-transport theory, in which

$$\langle c' \mathbf{u}' \rangle = -\mathbf{K} \nabla \langle c \rangle \tag{6-5}$$

where **K** is a (3 x 3) turbulent diffusivity tensor whose elements can be estimated from the output of a meteorological model or inferred from meteorological measurements.

Lamb (1973) evaluated the conditions of validity of Equation 6-5. He concluded that *K*-theory is applicable only when $\tau_e/T_c \ll 1$, where τ_e is the maximum time over which an average atmospheric turbulent eddy maintains its integrity and T_c is the time scale of the $\langle c \rangle$ field, i.e., $\partial \langle c \rangle / \partial t \simeq \langle c \rangle / T_c$. Therefore, the *K*-theory is applicable when the changes in the mean concentration field $\langle c \rangle$ have a larger scale than that of turbulent transport, a condition that is commonly violated near strong isolated sources (where T_c is short), especially with large wind direction horizontal meandering or unstable conditions (i.e., large τ_e).

The assumption of Equation 6-5 has, then, a limited applicability and has shown major limitations, especially for the treatment of point sources in unstable conditions. More complex formulations (higher order closure schemes) have been proposed for evaluation $\langle c'\mathbf{u}' \rangle$ and are discussed in Section 6.5.1.

Equation 6-4, with the assumption of Equation 6-5, is generally further simplified by assuming that (1) the tensor **K** is diagonal; (2) the molecular diffusion is negligible; and (3) c represents the concentration of a nonreactive pollutant (i.e., $\langle S \rangle = S$, as discussed below). With these simplifications, Equation 6-4 becomes the "semiempirical equation of atmospheric diffusion,"

$$\frac{\partial \langle c \rangle}{\partial t} = -\bar{\mathbf{u}} \cdot \nabla \langle c \rangle + \nabla \cdot \mathbf{K} \nabla \langle c \rangle + S \tag{6-6}$$

where the elements of **K** are zero, except along its main diagonal (K_{11}, K_{22}, K_{33}). Equation 6-6 can be integrated (analytically or numerically) if the inputs $\bar{\mathbf{u}}$, **K** and S are provided, together with initial and boundary conditions for $\langle c \rangle$.

In the case of a single source in stationary (i.e., $\partial < c > / \partial t = 0$) emission and meteorological conditions, the source term is commonly treated as an upwind boundary condition. For an average wind speed $\bar{u}$(x,y,z) blowing toward the positive x-axis, the following boundary condition applies in the upwind boundary plane (y,z):

$$< c > = \frac{Q}{\bar{u}(0, y_s, z_s + \Delta h)} \delta(z - z_s - \Delta h)\, \delta(y - y_s) \tag{6-7}$$

where Q is the pollutant emission rate, z_s is the physical height of the source located in $(0,y_s)$, Δh is the plume rise, and δ is the Kronecker operator. Using this boundary condition and assuming a steady state, Equation 6–6 becomes simply

$$\bar{\mathbf{u}} \cdot \nabla < c > = \nabla \cdot \mathbf{K} \nabla < c > \tag{6-8}$$

The integration of either Equation 6–6 or Equation 6–8 requires a full specification of boundary conditions. Total reflection conditions are generally assumed at the ground and at the top of the computational domain (which is generally the top of the PBL); i.e.,

$$K_{33} \frac{\partial < c >}{\partial z} = 0 \tag{6-9}$$

which indicates a pollutant flux equal to zero. In order to consider dry deposition phenomena at the ground surface, the following condition is often assumed instead of Equation 6–9 at z = 0 (i.e., at ground level)

$$K_{33} \frac{\partial < c >}{\partial z} = V_d < c > \tag{6-10}$$

which indicates a nonzero pollutant flux, where V_d is the deposition velocity, which is a function of meteorological conditions (e.g., atmospheric stability), pollutant type and surface type. Measured deposition velocities for SO_2 are presented in Figure 6–4, while deposition velocity ranges for several gases are listed in Table 6–1.

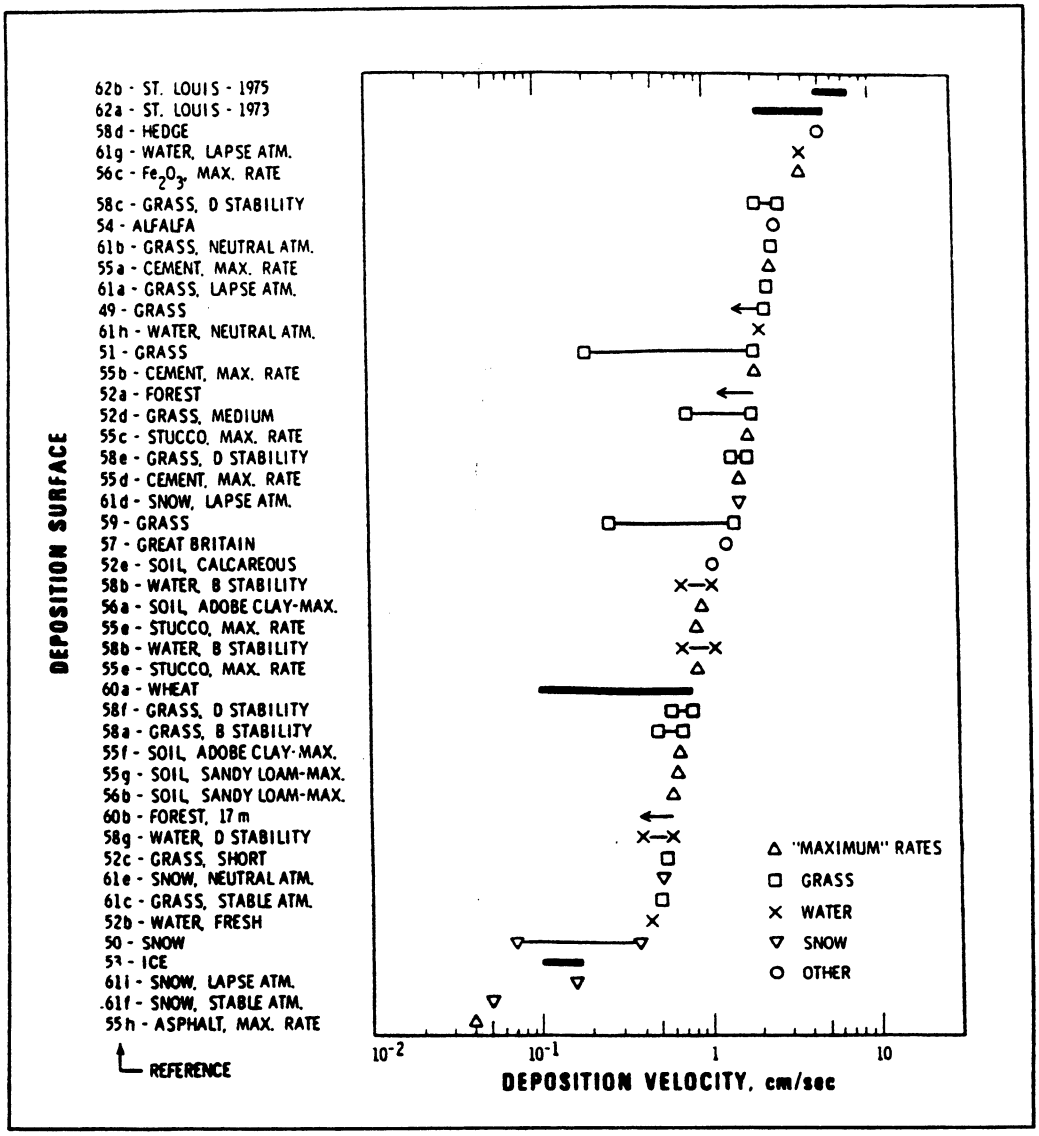

Figure 6–4. *SO_2 deposition velocity summary for different surfaces. From Sehmel (1980); see that paper for references mentioned in the figure. [Reprinted with permission from Academic Press.]*

Table 6–1. Deposition velocity range for gases. From Schmel (1980); see this paper for the references mentioned in the table. [Reprinted with permission from Academic Press.]

Number of references	Depositing gas	Deposition velocity range, cm s^{-1}
14	SO_2	0.04–7.5
20	I_2	0.02–26
2	HF	1.6–3.7
1	ThB	0.08–2.6
1	Fluorides	0.3–2.4
1	Cl_2	1.8–2.1
7	O_3	0.002–2.0
1	NO_2	1.9
2	NO	Minus–0.9
1	PAN	0.8
3	NO_x	Minus–0.5
1	H_2S	0.015–0.38
1	CO_2	0.3
1	$(CH_3)_2S$	0.064–0.28
5	CH_3I	$10^{-4} - 10^{-2}$
1	Kr	2.3×10^{-11} max

On the sides (x,z) and (y,z) of the computational domain, it is generally assumed

$$<c> = 0 \tag{6–11}$$

or

$$<c> = \textit{background value} \tag{6–12}$$

or (Shir and Shieh, 1974)

$$\nabla_h^2 <c> = 0 \tag{6–13}$$

where ∇_h is the horizontal Laplacian operator $\nabla_h^2 = \partial^2/\partial x^2 + \partial^2/\partial y^2$. The latter condition, Equation 6–13, represents a linear extrapolation of the concentration field outside the boundary.

Initial conditions are also required for the interpretation of Equation 6–6, which is time–dependent, and are generally specified by Equations 6–11 or 6–12 throughout the entire computational domain or, in special cases (e.g., Runca, 1977), by a pseudoanalytical plume equation that provides the initial concentration field $<c>$ near the point source(s) and eliminates the difficulties related to the numerical approximation of the S function (i.e., the source term).

If chemical reactions are involved, the assumption $<S> = S$ is no longer valid, and the term $<S>$ must be investigated further. We can say that (using c_m instead of c for the concentrations of all species; where $m = 1, 2, \ldots M$) the source term is

$$S_{c_m} = E_{c_m} + R_{c_m} + P_{c_m} \qquad (6\text{–}14)$$

where $S_{c_m}(x,y,z,t)$ is the total rate of addition (or removal) of the m-th species; $E_{c_m}(x,y,z,t)$ is the direct emission of the m–th species (primary emission); $R_{c_m}(x,y,z,t)$ is the creation/removal term of the m–th species by chemical reactions and is a function of the meteorology (especially ambient temperature and solar radiation) and, in general, of the concentration of all pollutants c_1, $c_2, \ldots c_M$, in (x,y,z) at time t; and $P_{c_m}(x,y,z,t)$ is the removal term for c_m due to precipitation, and is a function of meteorological variables (such as precipitation rate) and the type m of species. Equation 6–14 does not include dry deposition, which is treated as a boundary condition by Equation 6–10.

The ensemble average $<S_{c_m}>$ is a function of $<R_{c_m}>$, which, in general, is a nonlinear function of $c_1, c_2, \ldots c_m$. Thus, the averaging process $<R_{c_m}>$ creates new additional variables of the type $<c_i' c_j'>$, with $i, j = 1, 2, \ldots M$. The most common approximation for avoiding the generation of these new variables is

$$< R_{c_m}(c_1, c_2, \ldots c_M) > \simeq R_{c_m}(<c_1>, <c_2>, \ldots <c_M>) \qquad (6\text{–}15)$$

Again, however, Lamb (1973) showed that the above approximation may be a crude one. His analysis of a simple second-order decay reaction

$$R_{cm} = -\beta\, c_m^2 = -\beta\,(<c_m> + c'_m)^2 \tag{6-16}$$

shows that the approximation of Equation 6-15, i.e.,

$$<R_{cm}> \simeq -\beta <c_m>^2 \tag{6-17}$$

is valid only when

$$\beta <c_{\max}>\ \tau_e << 1 \tag{6-18}$$

Equation 6-18 requires the decay process to be slow (i.e., a small β) compared with turbulent transport time scale. Many photochemical reactions, however, are quite fast and, therefore, do not allow this approximation.

Equations 6-6 or 6-8 can be solved in two ways:

1. by analytical methods, providing exact solutions
2. by numerical methods, providing approximate solutions

These two approaches are discussed below.

6.2 ANALYTICAL SOLUTIONS

Analytical solutions are available for the steady state Equation 6-8 under special, simplifying assumptions. The available formulations have been discussed by Pasquill and Smith (1983), Seinfeld (1986), and Tirabassi et al. (1986). In particular, Roberts (see Calder, 1949) obtained a two-dimensional solution for ground-level sources; Smith (1957) found a solution for elevated sources with $\bar{u}$ and K_z profiles following Schmidt's conjugate law; Rounds (1955) proposed a more general solution, which, however, turned out to be valid only for linear profiles of K_z; finally, Yeh and Huang (1975) and Demuth (1978) obtained a more general analytical solution, which is presented below. This latter solution has been incorporated into an organized computer package, KAPPA-G (Tirabassi et al., 1986), which allows the performance of three-dimensional steady-state simulations using the Gaussian formula for the treatment of horizontal diffusion (as proposed by Huang, 1979).

Remembering that in Equation 6–8 the wind $\bar{u}$ is assumed to blow towards the positive x–axis, we can use the notation

$$K_{11} = K_x \tag{6–20}$$

$$K_{22} = K_y \tag{6–21}$$

$$K_{33} = K_z \tag{6–22}$$

Therefore, Equation 6–8 can be written

$$\bar{u}\frac{\partial}{\partial x}c = \frac{\partial}{\partial z}\left(K_z\frac{\partial}{\partial z}c\right) + \frac{\partial}{\partial y}\left(K_y\frac{\partial}{\partial y}c\right) \tag{6–23}$$

with boundary conditions

$$c = \frac{Q}{\bar{u}(h_e)}\,\delta(z - h_e)\,\delta(y) \qquad \text{at } x = 0 \tag{6–24}$$

and

$$K_z\frac{\partial c}{\partial z} = 0 \qquad \text{at } z = 0,\ h \tag{6–25}$$

where h_e is the final effective height of the emission (i.e., $h_e = z_s + \Delta h$), h is the depth of the mixing layer, $y_s = 0$, and

$$\left|\bar{u}\frac{\partial}{\partial x}c\right| \gg \left|\frac{\partial}{\partial x}\left(K_x\frac{\partial}{\partial x}c\right)\right| \tag{6–26}$$

Equation 6–26 assumes that atmospheric dispersion along the x–axis is negligible in comparison to the transport term.

To integrate Equation 6–23 we define the crosswind integrated concentration

$$\bar{c}(x, z) = \int_{-\infty}^{+\infty} c(x, y, z)dy \tag{6–27}$$

We also make the following assumptions

$$\bar{u}(z) = u_0(z/h_0)^a \tag{6-28}$$

$$K_y(x, z) = \bar{u}(z)\, f(x) \quad (*) \tag{6-29}$$

$$K_z(z) = K_{z0}(z/h_0)^\beta \tag{6-30}$$

and

$$h = +\infty \tag{6-31}$$

where h_0 is the height at which u_0 and K_{z0} are measured (or evaluated) and $f(x)$ is any function of x. Then the solution of Equation 6-23 for ground level concentration ($z = 0$) is (Yeh and Huang, 1975)

$$\bar{c}(x, 0) = \frac{Q}{\lambda^\eta} \frac{1}{\Gamma(\gamma)} \frac{h^{\eta_0}}{u_0^\nu (x\, K_{z0})^\gamma} \exp\left[-\frac{u_0\, h_0^r\, h_e^\lambda}{\lambda^2\, K_{z0}\, x}\right] \tag{6-32}$$

where

$$\lambda = a - \beta + 2 \tag{6-33}$$

$$\nu = (1 - \beta)/\lambda \tag{6-34}$$

$$\gamma = (a + 1)/\lambda \tag{6-35}$$

$$\eta = (a + \beta)/\lambda \tag{6-36}$$

$$r = \beta - a \tag{6-37}$$

and Γ denotes the Gamma function.

With a finite mixing height (i.e., $h < +\infty$) and $h_e < h$ (and with the other assumptions unchanged), the solution of Equation 6-23 is (Demuth, 1978)

$$\bar{c}(x, 0) = \frac{2\, Q\, q\, h_0^a}{h^{a+1}\, u_0} \left\{ \gamma + R^p \sum_{i=1}^{\infty} \left[\frac{J_{\gamma-1}\,(\sigma_{\gamma(i)}\, R^q)\, \sigma_{\gamma(i)}^{\gamma-1}}{\Gamma(\gamma)\, J_{\gamma-1}^2\,(\sigma_{\gamma(i)})\, 2^{\gamma-1}} \right.\right. \cdot \left.\left. \exp\left(-\frac{\sigma_{\gamma(i)}^2\, q^2\, K_{z0}\, x}{h^\lambda\, h_0^r\, u_0}\right)\right]\right\} \tag{6-38}$$

(*) This particular assumption, however, will be used only for deriving Equation 6-44, below.

where

$$R = h_e/h \tag{6-39}$$

$$p = (1 - \beta)/2 \tag{6-40}$$

$$q = \lambda/2 \tag{6-41}$$

In Equation 6-38, J_γ (...) represents the Bessel function of the first kind and order γ, and $\sigma_{\gamma(i)}$ (i=1,2,...) are its roots, i.e., $J_\gamma(\sigma_{\gamma(i)}) = 0$.

The solutions given by Equations 6-32 and 6-38 represent the case when $z = 0$, i.e., the concentration is computed at ground level. If elevated integrated concentrations $\bar{c}(x,z)$ need to be evaluated, the new solution, for $h = +\infty$, is easily obtained from Huang (1979), giving

$$\bar{c}(x,z) = \frac{Q\,(z h_e)^p\, h_0^\beta}{\lambda\, K_{z0}\, x}\, exp\left(-\frac{u_0\, h_0^r\, (z^\lambda + h_e^\lambda)}{\lambda^2\, K_{z0}\, x}\right) I_{-\nu}\left(\frac{2\, u_0\, h_0^r\, (z\, h_e)^q}{\lambda^2\, K_{z0}\, x}\right) \tag{6-42}$$

where $I_{-\nu}$ (...) is the modified Bessel function of the first kind and order $-\nu$.

If $h < +\infty$, the integrated concentration $\bar{c}(x,z)$ is again obtained from Demuth (1978), giving

$$\bar{c}(x,z) = \frac{2\, Q\, q\, h_0^a}{h^{a+1}\, u_0}\left\{\lambda + \left(\frac{z\, R}{h}\right)^p \sum_{i=1}^{\infty}\left[\frac{J_{\gamma-1}(\sigma_{\gamma(i)}\, R^q)\, J_{\gamma-1}(\sigma_{\gamma(i)}(z/h)^q)}{J_{\gamma-1}^2(\sigma_{\gamma(i)})}\right.\right. \cdot \left.\left. exp\left(-\frac{\sigma_{\gamma(i)}^2\, q^2\, K_{z0}\, x}{h^\lambda\, h_0^r\, u_0}\right)\right]\right\} \tag{6-43}$$

Tirabassi et al. (1986) verified, analytically or numerically, that as $z \to 0$, the limit of Equations 6-42 and 6-43 gives Equations 6-32 and 6-38, respectively; and that, as h $\to +\infty$, the limit of Equations 6-38 and 6-43 gives Equations 6-32 and 6-42, respectively.

The above formulae deal with the crosswind integrated concentration $\bar{c}(x,z)$. If we want to calculate the three-dimensional concentration $c(x,y,z)$, horizontal diffusion needs to be included in a way that satisfies Equation 6-29. If we

assume that the plume has a Gaussian concentration distribution in the horizontal with lateral standard deviation $\sigma_y(x)$, we obtain

$$c(x,y,z) = \bar{c}(x,z)\,\frac{1}{\sqrt{2\pi}\,\sigma_y}\,exp\left(-\frac{y^2}{2\,\sigma_y^2}\right) \qquad (6\text{–}44)$$

Equation 6–44, together with any function $\bar{c}(x,z)$ previously derived, can be used for three-dimensional simulations, since the Gaussian assumption for horizontal diffusion gives

$$K_y = \frac{\bar{u}}{2}\,\frac{d\sigma_y^2}{dx} \qquad (6\text{–}45)$$

which satisfies the condition of Equation 6–29.

6.3 NUMERICAL SOLUTIONS

Numerical methods allow the computation of approximate solutions of Equations 6–6 and 6–8 using integration techniques such as

- finite difference methods
- finite element methods
- spectral methods
- boundary element methods
- particle methods

The reader should refer to books on numerical analysis for further discussion of the above numerical techniques.

Finite difference methods (Richtmyer and Morton, 1967) are the oldest technique. Although they possess several disadvantages, they still represent the major and most applied (and best understood) numerical tool for this type of applications. However, finite-difference approximation of the advection term $\bar{\mathbf{u}} \cdot \nabla\langle c\rangle$ always produces a diffusion-type error that artificially increases the

diffusion rates in the simulated concentration output. This numerical phenomenon can be easily understood by analyzing the one-dimensional version of the advection term, i.e.,

$$\frac{\partial c}{\partial t} = - \bar{u} \frac{\partial c}{\partial x} \tag{6-46}$$

With a simple first-order finite-difference scheme, we obtain

$$\frac{c_i^{t+1} - c_i^t}{\Delta t} = \bar{u}_i^t \frac{c_{i+1}^t - c_{i-1}^t}{2\,\Delta x} \tag{6-47}$$

where subscripts indicate spatial discretization (with a grid size Δx) and superscripts indicate time discretization (with interval Δt). The analysis of the truncation terms (Johnson et al., in Stern, 1986) shows that the error ϵ generated by the approximation of using Equation 5–47 instead of Equation 5–46 is

$$\epsilon = \frac{\bar{u}\,\Delta x}{2} (1 - \bar{u}\,\Delta t/\Delta x)\,(\partial^2 c/\partial x^2) \tag{6-48}$$

which is a diffusion-type term, with associated diffusity D_n equal to

$$D_n = \frac{\bar{u}\,\Delta x}{2} (1 - \bar{u}\,\Delta t/\Delta x) \tag{6-49}$$

The term D_n is proportional to the grid size Δx and, especially in regional modeling where grid sizes have typical values of 80 km, generates an artificial diffusion that can easily reach values of the same order of magnitude as (or even greater than) actual atmospheric diffusion, which makes model outputs almost meaningless. Several methods have been proposed to reduce this error (Egan and Mahoney, 1972; Runca and Sardei, 1975; Boris and Book, 1973, who proposed the SHASTA method; Pepper et al., 1979, who used cubic splines and chapeau functions; Zalesak, 1979, who extended the concept of flux corrected transport, FCT, to any number of dimensions; Lamb, 1983, who developed the BIQUINTIC method for his regional scale photochemical model; Orszag, 1971, who first introduced the pseudospectral method; etc.). Numerical evaluations of most of these methods by Chock and Dunker (1983) and Schere (1983) show that a "best" approach cannot be identified for all situations, and that some schemes, like SHASTA, which used to be widely used in photochemical simulation packages, produce unacceptably large amounts of artificial diffusion.

In spite of several shortcomings of K-theory and grid discretization, this approach plays a major role in air pollution simulations, especially when non-linear chemistry is required (as for the evaluation of O_3 impacts). One could argue that the errors introduced by this technique pale in comparison to the assumptions introduced by the Gaussian plume model discussed in Chapter 7.

While analytical solutions require special, simplified functional forms for **K** (i.e., power laws of the altitude z), numerical solutions can accommodate for virtually any function $\mathbf{K}(x,y,z,t)$. Several of these functions have been proposed for evaluating K_H, the horizontal eddy diffusivity (which assumes $K_{11} = K_{22} = K_H$ for any wind direction angle with the x-axis), and K_z the vertical eddy diffusivity.

6.3.1 The Vertical Diffusivity K_z

The vertical diffusivity K_z is generally specified as a function of the altitude z. For example, McRae et al. (1982) use

$$K_z = 2.5\, w_* \, z_i \left[k\frac{s}{z_i}\right]^{4/3} \left[1 - 15\left(\frac{z}{L}\right)\right]^{1/4} \qquad (6\text{–}50)$$

in the unstable surface layer (i.e., $0 \leq z/z_i < 0.05$) and

$$K_z = w_* \, z_i \, f(z/z_i) \qquad (6\text{–}51)$$

in the unstable PBL above the surface layer, where

$$f(z/z_i) = 0.021 + 0.408\left(\frac{z}{z_i}\right) + 1.351\left(\frac{z}{z_i}\right)^2 - 4.096\left(\frac{z}{z_i}\right)^3 + 2.560\left(\frac{z}{z_i}\right)^4 \qquad (6\text{–}52)$$

for $0.05 \leq \frac{z}{z_i} \leq 0.6$,

$$f(z/z_i) = 0.2\, exp\left[6 - 10\left(\frac{z}{z_i}\right)\right] \qquad (6\text{–}53)$$

for $0.6 \leq \frac{z}{z_i} \leq 1.1$, and

$$f(z/z_i) = 0.0013 \qquad (6\text{–}54)$$

for $\frac{z}{z_i} > 1.1$.

Therefore, the eddy diffusivity K_z is $\simeq 0$ for $z \simeq 0$ and $z > z_i$, and has a maximum ($\simeq 0.21\, w_* \, z_i$) when $z/z_i \simeq 0.5$, as shown in Figure 6–5.

In neutral conditions, Shir (1973) adopts

$$K_z = k\, u_* \, z \, exp(-8\, z f / u_*) \tag{6-55}$$

where f is the Coriolis parameter defined by Equation 3-3, while Myrup and Ranzieri (1976) propose,

$$K_z = k\, u_* \, z \tag{6-56}$$

in the surface layer (i.e., $z/z_i < 0.1$), and, above the surface layer,

$$K_z = k\, u_* \, z\, (1.1 - z/z_i) \tag{6-57}$$

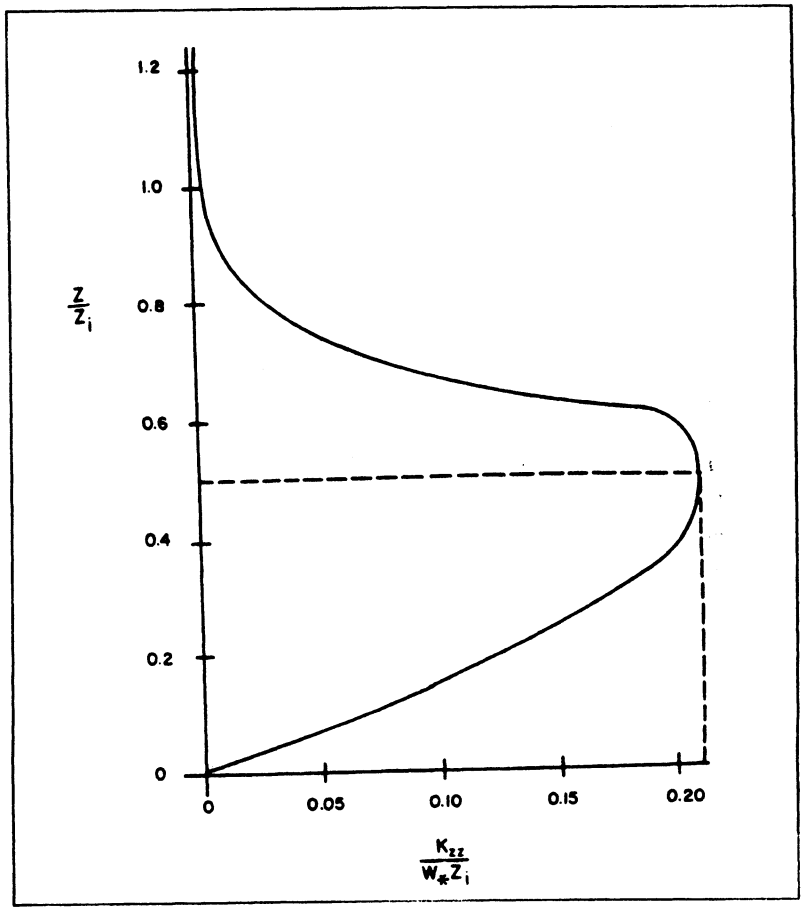

Figure 6-5. Vertical turbulent diffusivity profile under unstable conditions (from McRae et al., 1982). [Reprinted with permission from Academic Press.]

for $0.1 \leq z/z_i \leq 1.1$, and

$$K_z = 0 \tag{6-58}$$

for $z/z_i > 1.1$.

Finally, in stable conditions, Businger and Ayra (1974) propose

$$K_z = \frac{k\, u_* \, z}{0.74 + 4.7(z/L)} \exp\left(-\frac{8 f z}{u_*}\right) \tag{6-59}$$

More discussion about the evaluation of K_z can be found in Seinfeld (1986). It is clear, however, that we do not possess a definite knowledge of K_z above the surface layer and that the application of the K-theory to simulate vertical dispersion during unstable conditions is highly questionable.

6.3.2 The Horizontal Diffusivity K_H

The evaluation of K_H presents several intriguing aspects. It is often (and, perhaps, improperly) assumed that

$$K_H \simeq K_y \tag{6-60}$$

where K_y is the crosswind eddy diffusivity (i.e., with wind blowing along the positive x-axis). If we consider a plume originated at $x = 0$ and carried by the wind along the x-axis, K_y is related, through Equation 6-45, to the standard deviation $\sigma_y(x)$ of the crosswind plume concentration spread. where Equation 6-45 is valid for a travel time t, which is

$$t \gg T_L \tag{6-61}$$

where T_L is the Lagrangian time scale (typically of the order of 100–200 s). The integration of Equation 6-45 gives

$$\sigma_y(x) = \sqrt{2\, K_y\, x/\bar{u}} = \sqrt{2\, K_y\, t} \tag{6-62}$$

which would require σ_y to grow linearly with $x^{0.5}$. But the analysis of data on horizontal dispersion does not confirm Equation 6-63, as illustrated in Figure 6-6. These data show a peculiar property of atmospheric horizontal diffusion, i.e., its accelerating rate. This phenomenon, whose rate can be justified only partially by the theoretical analysis of Taylor (1921), seems to suggest

(Gifford, 1982) that atmospheric diffusion is augmented by the presence of large scale quasihorizontal turbulent wind-field heterogeneities, caused by large-scale surface inhomogeneities of various kinds.

Figure 6-6 clearly shows that the choice of K_y (or K_H) strongly depends upon the travel time t by several orders of magnitude. This creates the paradox that, if we want to estimate K_H in a certain location (x,y,z), for example the center of a grid cell, different values of K_H would be required for the different pollutants coming from different sources, and therefore, having different travel times. An Eulerian grid model cannot really handle this, since, after pollutants are injected into the grid cells, the memory of their different origin is lost. This entire discussion points out a further limitation of K-theory in describing atmospheric diffusion.

Another disturbing aspect of the numerical interpretation of the K-theory equation to simulate horizontal diffusion is that the effective eddy diffusion is the sum of K_H plus the contribution D_n generated by the numerical advection errors (a diffusion term, as explained at the beginning of Section 6.3). In many cases, $D_n > K_H$, which may explain (McRae et al., 1982) why the influence of changes in K_H in the large range 0-500 $m^2 s^{-1}$ is small in the concentration field, as presented by Liu et al. (1976). Due to the numerical error D_n, a K-theory model needs to use nonzero K_H values only during unstable conditions, in which, for example, we can use the formula

$$K_H \simeq 0.1\, w_* \, z_i \simeq 0.1\, z_i^{3/4} \, (-k\, L)^{-1/3} \, u_* \qquad (6\text{-}63)$$

derived from the measurements of Willis and Deardorff (1976).

A final important consideration about K_H derives from the definition of Equation 6-2, in which the wind vector $\mathbf{V}$ is divided into two components, $\overline{\mathbf{u}}$ and $\mathbf{u}'$, where $\overline{\mathbf{u}}$ represents the large portion of the flow that is resolvable using meteorological measurements or models and $\mathbf{u}'$ is the remaining unresolvable component. Clearly, the better the meteorological model or the interpolation of the measurements, the higher the time- and space-resolution of the term $\overline{\mathbf{u}}$ and the smaller the $|\mathbf{u}'|$ values.

This interpretation of Equation 6-2 is very important since that equation is often used to indicate an *intrinsic* property of the atmospheric motion (an average term plus turbulent fluctuation) instead of being interpreted as the sum of a resolvable and unresolvable component. This is a key issue in understanding the turbulent diffusion terms $\langle c'\mathbf{u}' \rangle$ which have been approximated using the

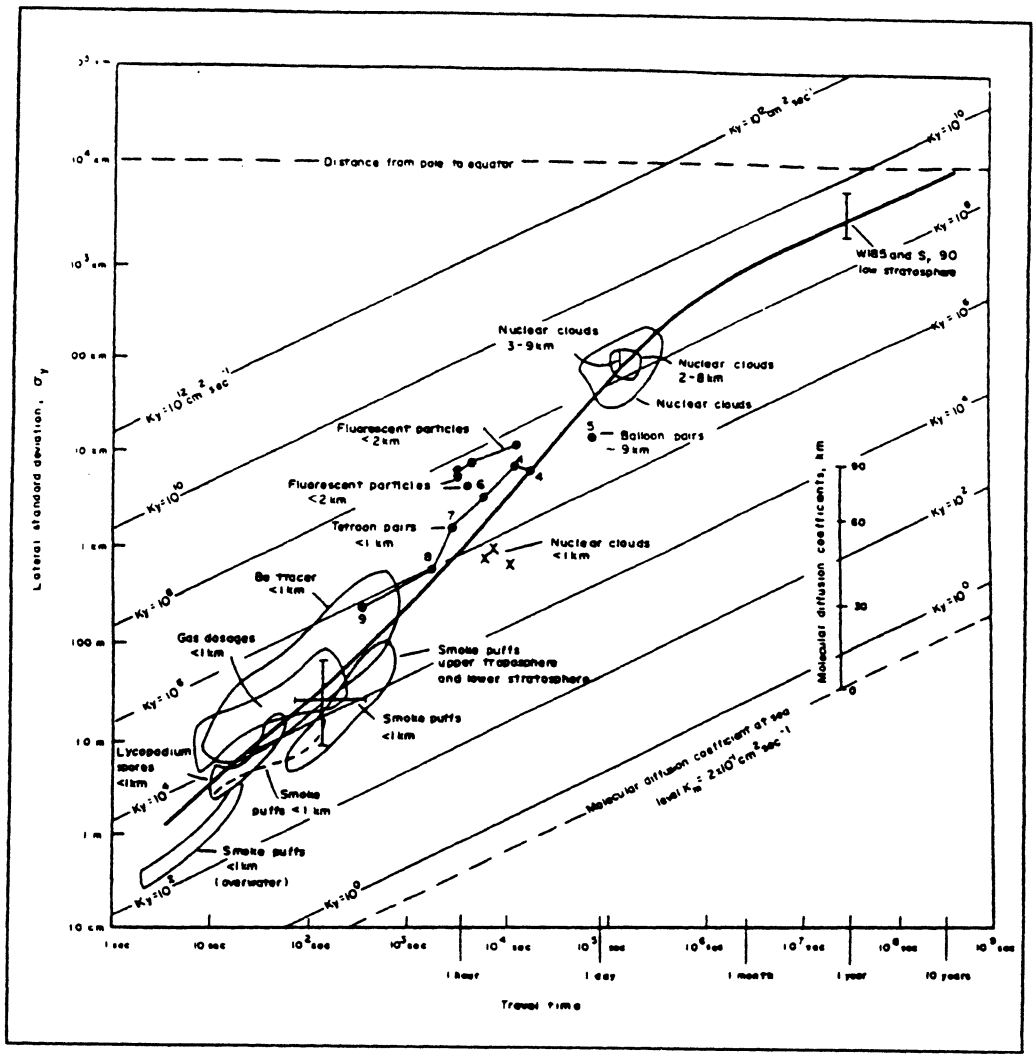

Figure 6–6. Summary of data on horizontal atmospheric diffusion, from Hage and Church (1967), as presented by Gifford (1982). The solid curve illustrates the empirical equation of Hage et al. (1967). [Reprinted with permission from Academic Press.]

K–theory by Equation 6–5, where **K** is a (3 x 3) turbulent diffusivity tensor. From the previous definition of $\mathbf{u}'$, it is clear that the better the meteorological model providing $\bar{\mathbf{u}}$, the lower the $|\langle c'\mathbf{u}'\rangle|$ terms and, consequently, the lower the magnitude of the elements of **K**. In other words, we derive the important (and, to a certain extent, surprising) conclusion that the eddy diffusion coefficients to be used in a diffusion model are a *function of the degree of performance* of the meteorological model used to calculate the meteorological input to the dispersion

model. This is particularly true for horizontal dispersion, since vertical velocity components are generally small in comparison with horizontal transport and, consequently, $\mathbf{u}'$ has a larger horizontal than vertical component.

In order to understand and fully evaluate the consequences of the above considerations, let us discuss a brief example related to long-range transport and horizontal diffusion of a plume from a point source. According to Hanna et al. (1977) and Irwin (1979), for downwind distances x greater than 10 km, the horizontal plume standard deviation σ_y is

$$\sigma_y = 33.3\, \sigma_\theta\, x^{1/2} \tag{6-64}$$

where σ_θ is the standard deviation of the horizontal wind direction expressed in radians. Using Equations 6-62 and 6-64, we obtain

$$K_y = 10^3\, \sigma_\theta^2\, u/2 \simeq K_H \tag{6-65}$$

For typical values of $\sigma_\theta < 0.5$ radians and u < 10 m/s, Equation 6-65 gives K_H values one to two orders of magnitude lower than the bottom of the range of $K_H = 10^4$ to 10^7 m^2 s^{-1} currently used in most long-range models and considered to be the best values to fit actual measurements. This inconsistency can be easily explained using the considerations presented before. In fact, Equations 6-64 and 6-65 implicitly assume that the plume trajectory is known exactly and that σ_y (and K_H) characterize only the plume horizontal growth *and not the uncertainty in plume location*. Actual modeling simulations, however, use or calculate meteorological wind fields, which possess a large degree of uncertainty when used for trajectory computations. Therefore, it is not surprising that actual model calibration tests suggest large values of K_H (10^4 to 10^7 m^2 s^{-1} instead of 10^2 to 10^3 m^2 s^{-1}). This indicates that horizontal diffusion needs to be artificially enhanced for the model to incorporate the uncertainties in the meteorological modeling computation of $\bar{\mathbf{u}}$.

In order to visualize the above considerations, let us consider the simple example in Figure 6-7, in which the contributions of three air pollution sources (S_1, S_2, and S_3) at the receptor R are evaluated through a dispersion model using large K_H values. Even though the model largely overestimates horizontal diffusion, it provides a total concentration value at R (the sum of the three dashed curves) that is quite similar to the measured value (on the solid curve), due to error compensation factors. The model is, in a way, "validated," but its

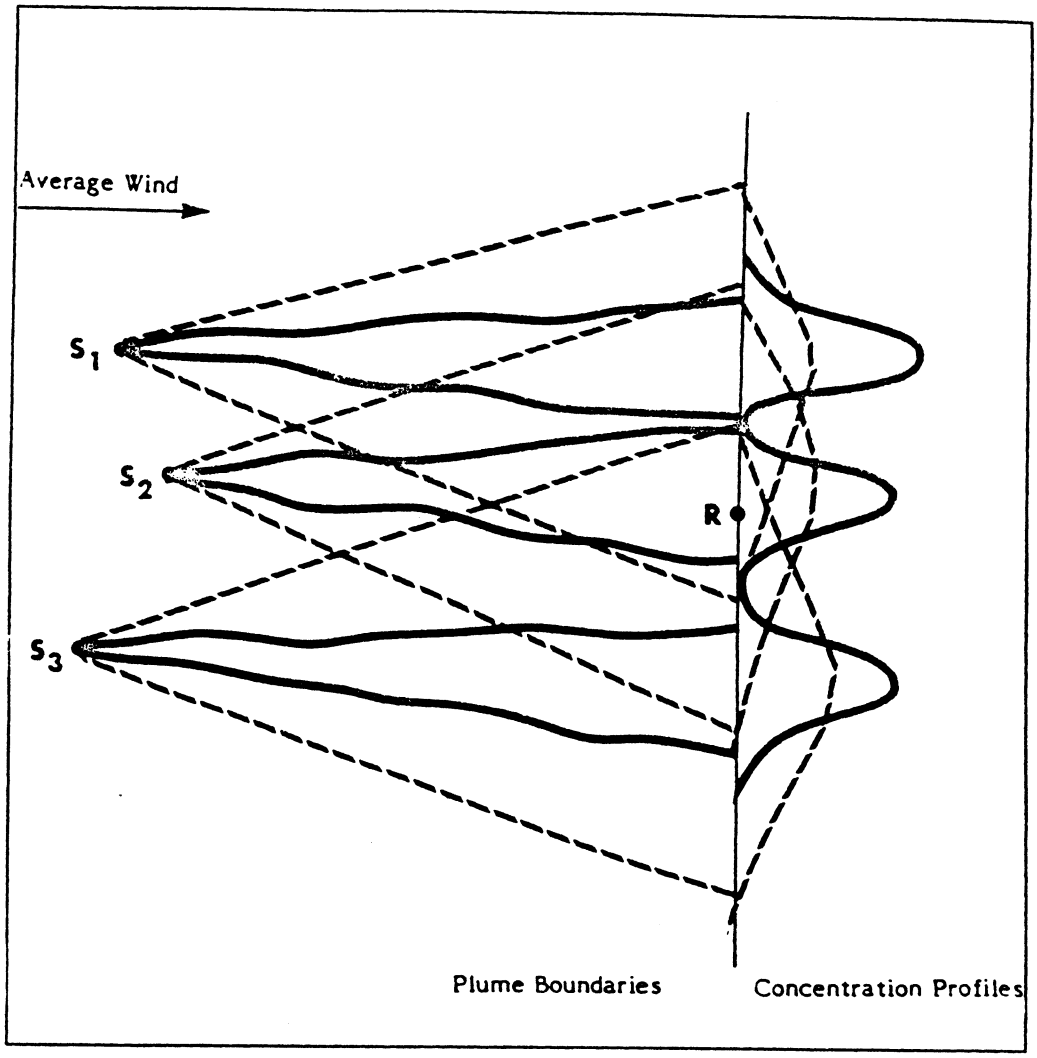

Figure 6–7. An example of the consequence of overestimating horizontal diffusion on the concentration at the receptor R. Solid lines show the actual average plume, while dotted lines show the plume as simulated by the model.

use for evaluating emission reduction strategies will provide incorrect results; specifically, it will suggest useless emission reductions in S_1 and S_3 and insufficient control of S_2.

It is true that regular fluctuations in wind direction cause the solid plumes in Figure 6–7 to sweep around the azimuth in such a way that they all may envelop the receptor R. This variation of the short-term average wind can

sometimes be correctly simulated, for long-term averages, by the dashed plumes, which are computed with an enhanced horizontal diffusion. However, wind direction fluctuations often do not show regular behavior and, therefore, do not support the above approximation. In complex terrain, especially, preferred direction patterns play important roles in determining plume trajectories, and the artificial enhancement of horizontal diffusion for long-term averages may provide incorrect results. Moreover, if nonlinear chemical reactions are used, the formation of secondary pollutants is incorrectly computed when the plume is diffused with artificially high dispersion rates, since the centerline plume concentration is consistently underestimated.

This discussion, which is valid only for the particular location of the receptor R, can, however, be generalized to illuminate a critical problem in most long-range air pollution modeling studies using K-theory grid models. In order to compensate for uncertainties in wind direction information, these models almost always over-estimate horizontal diffusion in a process that smoothes concentration peaks. With "smooth" emission source terms and wind frequency distributions, this assumption is quite acceptable, but, in many cases, this smoothing process creates a loss of deterministic information related to the source-receptor relationship. This loss becomes particularly critical when selective emission reduction strategies are inferred from modeling outputs in order to meet air quality goals at the receptor R.

6.4 BOX MODELS

6.4.1 The Single Box Model

The single box model (Lettau, 1970) is the simplest air pollution model and is based on the mass conservation of pollutant inside an Eulerian box, which generally represents a large area such as a city. The physical concept underlying the box model approach is depicted in Figure 6-8. Mass conservation gives

$$\frac{\partial}{\partial t}(c\, z_i) = Q - c\, z_i \frac{u}{\Delta x} \tag{6-66}$$

which, by integration, gives (Venkatram, 1978)

$$c(t)\, z_i(t) = c(t_o)\, z_i(t_o) \exp(-t/T_f) + Q\, T_f\, (1 - \exp(-t/T_f)) \tag{6-67}$$

If the dynamics of $z_i(t)$ are known, Equation 6–67 allows the computation of $c(t)$. In stationary conditions (i.e., $t = \infty$), c tends to the limit

$$c(\infty) = Q\,T_f/z_i \tag{6–69}$$

which is sometimes a reasonable quasistationary assumption in urban studies.

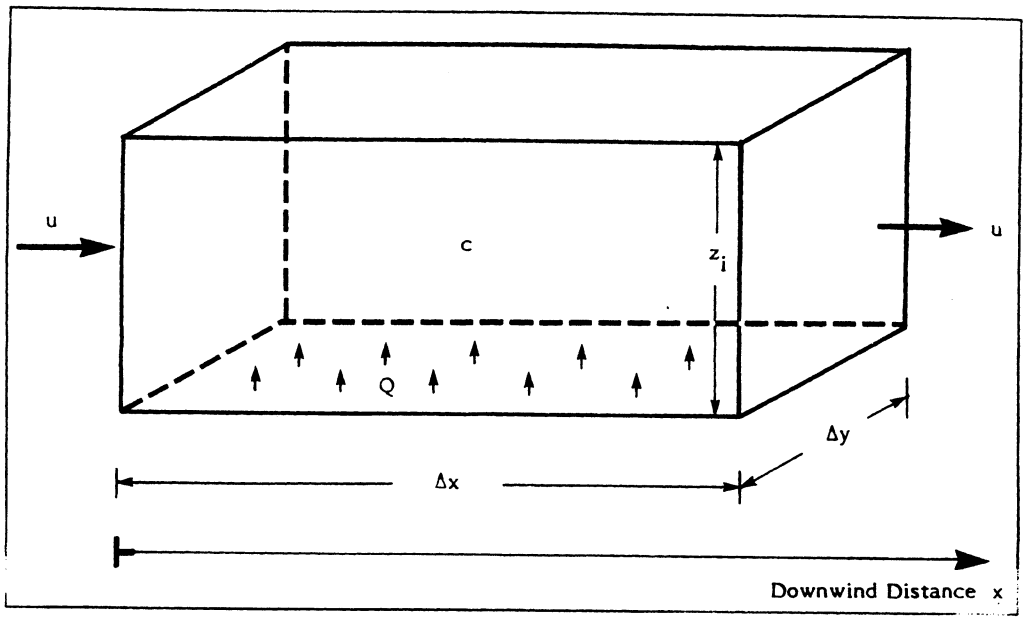

Figure 6–8. The single box model; z_i indicates the time varying mixing height, Δx and Δy are the horizontal dimensions of the box (e.g., the size of the city under investigation), Q is the constant emission for unit of area, c is the time–varying average concentration inside the box, and u is the constant wind speed injecting clean air into the box.

The single box model has frequently been applied for both inert and reactive pollutants; in the latter case, Equation 6–66 has to be modified to incorporate a chemistry module in the mass–balance computations. As a particular example of its application, Meszaros et al. (1978) used a box model for computing the atmospheric sulfur budget over Europe and incorporated both natural/anthropogenic emissions and dry/wet deposition in Equation 6–66. Also, Jensen and Peterson (1979), who used an acoustic sounder for evaluating $z_i(t)$, found good agreement between the single box model output $c(t)$ and urban concentration measurements.

anthropogenic emissions and dry/wet deposition in Equation 6–66. Also, Jensen and Petersen (1979), who used an acoustic sounder for evaluating $z_i(t)$, found good agreement between the single box model output $c(t)$ and urban concentration measurements.

6.4.2 The Slug Model

Venkatram (1978) showed that the box model has a great deal of inertia and cannot properly handle rapid temporal changes in either Q or u. He proposed the slug model as an improvement of the box model, especially during stagnation episodes. The slug model allows the concentration c to vary in the along-wind direction x and in the vertical direction z, but assumes that the concentration does not vary in the crosswind direction y. This allows us to write the mass-conservation equation within the single box in terms of two dimensions (x, z) as

$$\frac{\partial(c\, z_i)}{\partial t} + u\,\frac{\partial(c\, z_i)}{\partial x} = Q \tag{6–70}$$

where x is the downwind distance inside the box. We define the average concentration at x to be $\bar{c}(x)$, where

$$\bar{c}(x)\, z_i(x) = \int_0^{z_i(x)} c(x, z)\, dz \tag{6–71}$$

and $z_i(x)$ is either the mixing height or the vertical size (growing with x) of the "urban plume" generated by the ground level emission Q.

The solution of Equations 6–70 and 6–71 after the emission is shut off (i.e., after Q becomes zero) is

$$\bar{c}(x, t) = (x - u\, t)\,\frac{Q}{z_i(x)} \tag{6–72}$$

for $t \leq x/u$, and

$$\bar{c}(x, t) = 0 \tag{6–73}$$

for $t > x/u$. For $t = T_f$, the above scheme properly gives $\bar{c} = 0$ throughout the entire box, whereas the single box solution of Equation 6–67 is not able to reproduce this complete flushing.

6.4.3 Multi-Box Models

The single box concept has been extended to multi-box simulations (e.g., Ulbrick, 1968; Reiquam, 1970; Gifford and Hanna, 1973). Johnson (in Stern, 1976) describes the multi-box model in its simplest form by the equation

$$\Delta c_{i,j} = [(F_{i-1/2,j} - F_{i+1/2,j}) + (F_{i,j-1/2} - F_{i,j+1/2}) + Q_{ij}\,\Delta t]/V \quad (6\text{–}74)$$

where $\Delta c_{i,j}$ is the variation of the average concentration $c_{i,j}$ in the box i, j during the time interval Δt; i, j are the box horizontal indices; $Q_{i,j}(t)$ is the pollutant emission rate from all sources inside the box; and V is the volume of the box (i.e., $V = \Delta x\ \Delta y\ h$, where h is the height of the box above the ground). F represents the pollutant flux through the sides of the box; i.e.,

$$F_{i\pm1/2,j} = c_{i,j}\,A_{i\pm1/2,j}\,u_{i\pm1/2,j} \quad (6\text{–}75)$$

$$F_{i,j\pm1/2} = c_{i,j}\,A_{i,j\pm1/2}\,u_{i,j\pm1/2} \quad (6\text{–}76)$$

where A is the area of the side of the box, u the wind velocity component perpendicular to A, and the 1/2 term in the indices indicates the side between one cell and the other (e.g., i+1/2 means between i and i+1, and j–1/2 means between j–1 and j).

The two major limitations of this multi-box approach are its neglect of horizontal dispersion and the assumption of instantaneous mixing throughout the box (especially in the vertical). It is, however, computationally fast and, in several cases, may provide satisfactory, cost-effective answers, especially in regions in which detailed meteorological and emission information is not available.

6.5 ADVANCED EULERIAN MODELS

Because of the several shortcomings of the K-theory described in the previous sections, more complex Eulerian formulations for simulating atmospheric diffusion have been proposed. Among them, two have received particular attention: second-order closure modeling (e.g., Lewellen and Teske, 1976) and large eddy simulation techniques (e.g., Nieuwstadt and de Valk, 1987).

6.5.1 Second-Order Closure Modeling

Instead of using the K-theory approximation of Equation 6–5, an exact equation (Donaldson, 1973) can be computed for the second-order correlations

$\langle c'\mathbf{u}'\rangle$. This equation, however, introduces new variables, other than second-order correlations, that leave the system undetermined. A second-order closure model finds a relation between these new variables and the previous ones (i.e., the second-order correlations and the mean flow variables). Using this approach, Lewellen and Teske (1976) obtained a partial differential equation for the turbulent mass flux that has a dual behavior: for the initial plume, characterized by a plume scale that is smaller than the ambient turbulence scale, the equation shows hyperbolic behavior, while, for larger plume scales, the equation shows a smooth transition to parabolic behavior. Only the latter feature can be described well by the K-theory.

The model of Lewellen and Teske (1976) was successfully compared with laboratory simulations (Deardorff and Willis, 1974) of diffusion in convective conditions. The model was able to predict the rise of the maximum concentration from the ground. Comparisons with data collected during tracer experiments, however, were less encouraging (Lewellen and Sykes, 1983) and neither the patterns nor the magnitude of plume concentrations were correctly predicted. Therefore, the practical applicability of higher-order closure models is still questionable, even though some recent results (e.g., Enger, 1986) have shown encouraging features.

Second-order closure techniques have also been used to define new plume and puff methodologies. Sykes et al. (1989a) developed the Second-Order Closure Integrated Plume Model (SCIMP), the model with the lowest resolution in a hierarchy of models developed for EPRI. The model was tested against approximately 500 hours of plume data and seems to perform better than standard U.S. EPA regulatory models (such as MPTER). Sykes et al. (1989b) also developed the Second-Order Closure Integrated Puff model (SCIPUFF), the intermediate resolution member of the hierarchy of models mentioned above. The overall performance results of SCIPUFF were close to those obtained with SCIMP.

6.5.2 Large Eddy Simulation Models

As described by Nieuwstadt and de Valk (1987), a large eddy model such as those developed by Deardorff (1974) and Nieuwstadt et al. (1986), calculates the large-scale turbulent motions by directly solving a set of modified Navier-Stokes equations. These equations are

- a "filtered"(*) momentum equation with extra subgrid terms
- a "filtered" temperature equation with extra subgrid terms
- a Poisson equation for the pressure
- gradient transfer equations for the closure of all the extra terms describing the subgrid motions.
- an equation for the subgrid energy

These equations are solved (typically using finite-difference methods) with grids of about 50 to 100 m and time steps of about 5 s.

Using the output of the Deardorff (1974) model, Lamb (1978) successfully simulated the statistics of nonbuoyant particles in convective conditions. Nieuwstadt and de Valk (1987), instead, used a conservation equation for the contaminant, which is solved concurrently with the large eddy model. This second approach is able to replicate well the laboratory experiments by Willis and Deardorff (1981), who reproduced the behavior of a nonbuoyant contaminant in convective conditions. This good agreement was not recreated using a buoyant plume simulation and comparing it with the experiments of Willis and Deardorff (1983). However, further work by van Haren and Nieuwstadt (1989) shows a reasonable agreement between the output of the large eddy simulation model and the buoyant plume field experiments performed by Carras and Williams (1984).

In conclusion, large eddy simulation models seem promising and represent the approach that is closest to the recreation of the physics of atmospheric diffusion. Their simulation of buoyant plumes, however, needs further study. Also, it is possible that other computational techniques, such as Monte-Carlo Lagrangian particle models (see Chapter 8), will be able to show similar simulation ability at a lower computational cost, by reproducing the main stochastic behavior of atmospheric motion without explicitly solving the Navier-Stokes equations.

(*) By "filtering," we mean the elimination of the small-scale motions that are smaller than the numerical grid.

REFERENCES

Boris, J., and D.L. Book (1973): Flux-corrected transport. I. SHASTA, a fluid transport algorithm that works. *J. Comput. Phys.*, **12**:38–69.

Businger, J.A., and S.P. Ayra (1974): Heights of the mixed layer in the stable, stratified planetary boundary layer. *Adv. Geophys.*, **18A**:73–92.

Calder, K.L. (1949): Eddy diffusion and evaporation in flow over aerodynamically smooth and rough surfaces: A treatment based on laboratory laws of turbulent flow with special reference to conditions in the lower atmosphere. *Quart. J. Mech. Math.*, **2**:153.

Carras, J.N., and D.J. Williams (1984): Experimental studies of plume dispersion in convective conditions – 1. *Atmos. Environ.*, **18**:135–144.

Chock, D.P., and A.M. Dunker (1983): A comparison of numerical methods for solving the advection equation. *Atmos. Environ.*, **17**(1):11–24.

Deardorff, J.W., and G.E. Willis (1974): Physical modeling of diffusion in the mixed layer. *Proceedings*, Symposium on Atmospheric Diffusion Air Pollution sponsored by the American Meteorological Society, Santa Barbara, California, September.

Deardorff, J.W. (1974): Three-dimensional numerical study of the height and mean structure of a heated planetary boundary layer. *Boundary-Layer Meteor.*, **7**:81–106.

Demuth, C. (1978): A contribution to the analytical steady solution of the diffusion equation for line sources. *Atmos. Environ.*, **12**:1255–1258.

Donaldson, C. duP. (1973): Construction of a dynamic model of the production of atmospheric turbulence and the dispersal of atmospheric pollutants. *Proceedings*, Workshop on Micrometeorology sponsored by the American Meteorological Society, Boston, pp. 313–392.

Egan, B.A., and J.R. Mahoney (1972): Numerical modeling of advection and diffusion of urban area source pollutants. *J. Appl. Meteor.*, **11**:312–322.

Enger, L. (1986): A higher order closure model applied to dispersion in a convective PBL. *Atmos. Environ.*, **20**:879–894.

Gifford, F.A., and S.R. Hanna (1973): Modeling urban air pollution. *Atmos. Environ.*, **7**:131–136.

Gifford, F.A. (1982): Horizontal diffusion in the atmosphere: a Lagrangian-dynamical theory. *Atmos. Environ.*, **16**:505–512.

Hage, K.D., P.S. Brown, G. Arnason, S. Lazorick, and M. Levitz (1967): A computer program for the fall and dispersion of particles in the atmosphere. Sandia Corporation Report SC-CR-67-2530, The Travelers Research Center, Inc.

Hage, K.D., and H.W. Church (1967): A computer-programmed model for calculation of fall and dispersion of particles in the atmosphere. *Proceedings*, USAEC Meteor. Info. Meeting, Chalk River Nuclear Labs., 11–14 Sept. 1967, pp. 320–333. Atomic Energy of Canada, Ltd., Report AECL-2787.

Hanna, S.R., et al. (1977): AMS Workshop on Stability Classification Schemes and Sigma Curves — Summary of Recommendations. *J. Climate and Appl. Meteor.*, **58**(12):1305–1309.

Huang, C.H. (1979): A theory of dispersion in turbulent shear flow. Atmos. Environ., **13**:*453–463*.

Irwin, J.S. (1979): Estimating plume dispersion — A recommended generalized scheme. Presented at 4th Symposium on Turbulence and Diffusion, sponsored by the American Meteorological Society, Reno, Nevada.

Jensen, N.O., and E.L. Petersen (1979): The box model and the acoustic sounder, a case study. *Atmos. Environ.*, **13**:717–720.

Lamb, R.G. (1973): Note on application of K-theory to turbulent diffusion problems involving chemical reaction. *Atmos. Environ.*, **7**:235.

Lamb, R.G. (1978): A numerical simulation of dispersion from an elevated point source in the convection layer. *Atmos. Environ.*, **12**:1297–1304.

Lamb, R.G., and D.R. Durran (1978): Eddy diffusivities derived from a numerical model of the convective planetary boundary layer. *Nuovo Cimento*, **1C**:1–17.

Lamb, R.G. (1983): A regional scale (1000 km) model of photochemical air pollution. Part I, Theoretical formulation. U.S. EPA Document EPA–600/3–83–035. Research Triangle Park, North Carolina.

Lettau, H.H. (1970): Physical and meteorological basis for mathematical models of urban diffusion processes. *Proceedings*, Symposium on Multiple-Source Urban Diffusion Models. U.S. EPA Publication No. AP–86.

Lewellen, W.S., and M.E. Teske (1976): Second-order closure modeling of diffusion in the atmospheric boundary layer. *Boundary-Layer Meteor.*, **10**:69–90.

Lewellen, W.S., and R.I. Sykes (1983): Second-order closure model exercise for the Kincaid Power Plant Plume. Electric Power Research Institute Report EA–1616–9, Palo Alto, California.

Liu, M.-K., D.C. Whitney, and P.M. Roth (1976): Effects of atmospheric parameters on the concentration of photochemical air pollutants. *J. Appl. Meteor.*, **15**:829–835.

Longhetto, A., Ed. (1980): *Atmospheric Planetary Boundary Layer Physics*. New York, Elsevier.

McRae, G.J., W.R. Goodin, and J.H. Seinfeld (1982): Mathematical modeling of photochemical air pollution. Environmental Quality Laboratory Report No. 18, Pasadena, California. Also see: McRae, G.J., W.R. Goodin, and J.H. Seinfeld (1982): Development of a second generation mathematical model for urban air pollution. I. Model formulation. *Atmos. Environ.*, **16**(4):679–696.

Meszaros, E., G. Varhelyi, and L. Haszpra (1978): On the atmospheric sulfur budget over Europe. *Atmos. Environ.*, **12**:2273–2277.

Myrup, L.O., and A.J. Ranzieri (1976): A consistent scheme for estimating diffusivities to be used in air quality models. California Department of Transportation Report CA-DOT-TL-7169-3-76-32, Sacramento.

Nieuwstadt, F.T., and H. van Dop, Eds. (1982): *Atmospheric Turbulence and Air Pollution Modeling*. Dordrecht, Holland: Reidel.

Nieuwstadt, F.T., R.A. Brost, and T.L. van Stijn (1986): Decay of convective turbulence, a large eddy simulation. *Proceedings*, 199 Euromech meeting on Direct and Large Eddy Simulation of Turbulence, Munchen, 1985, Braunschweig/Weisbaden, Germany: Friedr. Vieweg & Sohn.

Nieuwstadt, F.T., and J.P. de Valk (1987): A large eddy simulation of buoyant and non-buoyant plume dispersion in the atmospheric boundary layer. *Atmos. Environ.*, **21**(12):2573-2587.

Orszag, S.A. (1971): Numerical simulation of incompressible flows within simple boundaries. I. Galerkin (spectral) representations. *Stud. Appl. Math.*, **50**:293-326.

Pasquill, F., and F.B. Smith (1983): *Atmospheric Diffusion*, Third Edition. New York: Halsted Press, John Wiley and Sons.

Pepper, D.W., C.D. Kern, and P.E. Long, Jr. (1977): Modeling the dispersion of atmospheric pollution using cubic splines and Chapeau functions. *Atmos. Environ.*, **13**:223-237.

Reiquam, H. (1968): *Atmos. Environ.*, **4**:233.

Richtmyer, R.D., and K.W. Morton (1967): *Difference Methods for Initial-Value Problems*. New York: Interscience Publications, John Wiley & Sons.

Rounds, W. (1955): Solutions of the two-dimensional diffusion equation. *Trans. Am. Geophys. Union*, **36**:395.

Runca, E., and F. Sardei (1975): Numerical treatment of the dependent advection and diffusion of air pollutants. *Atmos. Environ.*, **9**:69-80.

Runca, E. (1977): Transport and diffusion of air pollutants from a point source. *Proceedings*, IFIP Working Conference on Modeling and Simulation of Land, Air and Water Resource System, Ghent, The Netherlands.

Schere, K.L. (1983): An evaluation of several numerical advection schemes. *Atmos. Environ.*, **17**:1897-1907.

Sehmel, G. (1980): Particle and gas dry deposition: A review. *Atmos. Environ.*, **14**:983.

Seinfeld, J.H. (1986): *Atmospheric Chemistry and Physics of Air Pollution*. New York: John Wiley & Sons.

Shir, C.C. (1973): A preliminary numerical study of atmospheric turbulent flows in the idealized planetary boundary layer. *J. Atmos. Sci.*, **30**:1327-1339.

Shir, C.C., and L.J. Shieh (1974): A generalized urban air pollution model and its application to the study of SO_2 distributions in the St. Louis metropolitan area. *J. Appl. Meteor.*, **13**:185-204.

Smith, F.B. (1957): The diffusion of smoke from a continuous elevated point source into a turbulent atmosphere. *J. Fluid Mech.*, **2**:49.

Stern, A.C., Ed. (1976): *Air Pollution*. 3rd Edition, Volume I. New York: Academic Press.

Sykes, R.I., W.S. Lewellen, S.F. Parker, and D.S. Henn (1989a): A hierarchy of dynamic plume models incorporating uncertainty. Volume 3: Second-order closure integrated model plume (SCIMP). A.R.A.P. Division of California Research & Technology, Inc., Final Report EA-1616-28, Vol. 3, Princeton, New Jersey.

Sykes, R.I., W.S. Lewellen, S.F. Parker, and D.S. Henn (1989b): A hierarchy of dynamic plume models incorporating uncertainty. Volume 4: Second-order closure integrated puff. A.R.A.P. Division of California Research & Technology, Inc., Final Report EA-6095, Vol. 4, Princeton, New Jersey.

Taylor, G.I. (1921): Diffusion by continuous movements. *Proceedings*, London Math. Soc., **20**: 196-211.

Tirabassi, T., M. Tagliazucca, and P. Zannetti (1986): KAPPA-G, a non-Gaussian plume dispersion model: Description and evaluation against tracer measurements. *JAPCA*, **36**:592-596.

Ulbrick, E.A. (1968): *Socio-Encon. Plan. Sci.*, 1:423.Venkatram, A. (1978): An examination of box models for air quality simulation. *Atmos. Environ.*, **12**:2243-2249.

van Haren, L., and F.T. Nieuwstadt (1989): The behavior of passive and buoyant plumes in a convective boundary layer, as simulated with a large-eddy model. *J. Appl. Meteor.*, **28**:818.

Willis, G.E., and J.W. Deardorff (1976): A laboratory model of diffusion into the convection planetary boundary layer. *Quart. J. Royal Meteor. Soc.*, **102**:427-445.

Willis, G.E., and J.W. Deardorff (1981): A laboratory study of dispersion from a source in the middle of the convectively mixed layer. *Atmos. Environ.*, **15**:109-117.

Willis, G.E., and J.W. Deardorff (1983): On plume rise within a convective boundary layer. *Atmos. Environ.*, **17**:2935-2447.

Yeh, G.T., and C.H. Huang (1975): Three-dimensional air pollutant modeling in the lower atmosphere. *Boundary-Layer Meteor.*, **9**:*381*.

Zalesak, S.T. (1979): Fully multidimensional flux-corrected transport algorithms for fluids. *J. Comput. Phys.*, **31**:335-362.